


Approach for the improvement of sensitivity and sensing speed of TFET-based biosensor by using plasma formation concept

Deepak Soni , Dheeraj Sharma, Mohd. Aslam, Shivendra Yadav

Nanoelectronics and VLSI Lab, Electronics and Communication Engineering Discipline, Indian Institute of Information Technology, Jabalpur 482005, India

✉ E-mail: deepaksoni09@gmail.com

Published in Micro & Nano Letters; Received on 31st May 2018; Revised on 7th August 2018; Accepted on 30th August 2018

In this work, a new design of dual-gate source electrode (SE) dielectric-modulated tunnel field-effect transistor (TFET) biosensor with improved sensitivity and sensing speed has been presented. For this, P+ (source) I (channel) N+ (drain) type conventional TFETs structure is initially considered for comparison. Further to this, for the first time, an additional electrode is placed over the physically doped source region of the conventional biosensor with the negative supply voltage for extension of the cavity over the source region. The use of extra SE with negative supply voltage for the formation of cavity over the source region overcome the issues related to the formation of abrupt junction (at source/channel junction) and solubility limit of silicon material by the formation of a plasma layer of holes near to Si/HfO₂ interface in the source region. Moreover, the presence of extra biomolecules in the source cavity region of the proposed device further increases the concentration of plasma layer of holes near to Si/HfO₂ due to better coupling of SE and source region which is responsible for the improvement in sensing capability and sensing the speed of TFET biosensor. In this concern, a comparative investigation has been performed.

1. Introduction: The sensitivity and sensing speed are the significant parameters of concern for the designing of a biosensor [1, 2]. The sensitivity of biomolecule detection increases as the device dimensions are scaled down. The field-effect transistor (FET)-based dielectric modulated biosensors proved itself as the most potential candidate for the design of the next-generation biosensor [3–5] but, FETs-based biosensor faces challenges like a limitation of scalability due to short-channel effect (SCE) and high subthreshold swing (SS) (>60 mV/decade) [6, 7]. Due to SCEs, miniaturisation of the device is not feasible for the further improvement of sensitivity of FET device and high SS of FET is responsible for the high response time of the FET-based biosensor device. In the FET devices for sensing the biomolecules, a cavity is carved in the dielectric material under the gate region. So the biomolecules are immobilised inside it [6–8]. The presence of biomolecule inside the cavity provides changes in the electrostatic coupling between gate and channel regions of the FET devices which creates an impact on the barrier of the source/channel interface [6–8]. The change in the barrier at source/channel interface is responsible for changes in the electrical parameter of the device and sensing of the biomolecules [7, 8]. The distribution of biomolecules inside the cavity is considered to be a continuum which is helpful in understanding the fundamental behaviour and operation. The actual biomolecules binding is quite different because the probes and target biomolecules are discrete entity [8]. The position of the hybridised probe/target pair is very important for sensitivity point of view, as the density of the probes increases near the source/channel junction it improves the sensitivity of the device [8].

Further, for the replacement of FETs, the tunnel FETs (TFETs) have been examined for biomolecule detection process due to distinct advantages such as low SS (<60 mV/decade), scalability, low power dissipation, and compatibility with existing (CMOS) technology [8, 9]. The sensing capability of TFET is higher in comparison to FET biosensor because TFET-based biosensor is not suffered from SCEs with the miniaturisation of device and tunnelling-based phenomenon at the source–channel junction. TFET has low SS due to band-to-band tunnelling (BTBT)

mechanism, which provides the low response time (time required to detect biomolecules) [10–12]. In case of TFET devices, a cavity is formed in the gate oxide region, which immobilised the biomolecules inside it and changes the electrical parameters, these variations show the sensitivity of TFET biosensor.

In the literature, the different techniques are explored to improve the sensing capability and sensing speed by the researchers such as nanogap cavity is created at the source side in conventional DG-TFET biosensor [10, 13–16] which modulate the coupling between gate electrode and channel regions and senses the biomolecule. The cavity created at the drain side which changes the ambipolar conduction and sense the biomolecule in the cavity region [17], short-gate full-gate TFET-based biosensor [18] where the short-gate device has higher sensitivity due to better coupling between the gate and channel regions.

To improve the performance of biosensor, a heavily doped *n*⁺-pocket and gate-to-source overlap is used in vertical tunnelling-based TFET biosensor [18], where lateral and vertical tunnelling phenomena are used to improve sensitivity. Still, the TFET-based biosensors suffer from low sensitivity and sensing speed, because of the restricted design of cavity and abruptness at the source–channel junction. The sensing speed can be improved by improving the abruptness at the source–channel junction but the abruptness at source–channel junction is limited by higher limit of physical doping in the source region, which is known as solubility limit, this limitation of silicon does not allow to dope the silicon beyond a certain limit. Thus, it is not possible to reduce the response time of the TFET device.

In this regard, a new design of TFET structure is presented for improving the sensitivity and sensing the speed of TFET-based biosensor. For this, a conventional PIN type structure is considered along with this, an additional electrode is placed over the source region with a negative supply voltage (–1.2 V). The negative voltage over source region induces the holes at the surface of the Si/HfO₂ interface, creates a plasma layer of the hole at the silicon/HfO₂ interface and overcomes the limitation of solubility. Holes layer at the interface in the source region creates abruptness at the source–channel junction, increases the drain current [19]. Further, the cavity in the proposed structure

is extended from the gate dielectric region to source dielectric region. Thus, as the molecules enter into the cavity it changes the coupling between the gate electrode and channel regions consequently electrical parameter changes and shows the sensitivity of the device. Along with this, improved dielectric constant under the source cavity region creates an abrupt junction profile, reduces the SS and lowers the response time of the device as the biomolecules enters into the cavity region. Because the electrical parameters are dependent upon gate as well as source region dielectric, therefore, the proposed device shows higher sensitivity and sensing speed in comparison to the conventional device.

The use of dielectrically-modulated TFETs for selective detection in the liquid phase has been proposed. In contrast, selective detection of chemical species in the gas phase has been rather limited [20, 21]. In this paper, we show that the application of TFET-based biosensor device parameters can provide high selectivity towards specific volatile organic compounds (VOCs) [20]. Implementation of TFET for selective detection in liquid phase has been presented. Functionalisation of TFET with amine/oxide, biotin, antigen, or calmodulin has allowed real-time selective (or specific) detection of pH, streptavidin, antibody, and calcium ions, respectively, in a liquid phase [20, 22, 23]. Also, functionalisation of TFETs with tyrosine kinase, antibody receptor, or peptide nucleic acids (PNAs) allowed the selective detection of Ab1 tyrosine kinase, influenza-A virus, or DNA, respectively, in biological samples [22, 23]. In these applications, the receptors attached to the TFET surface bind specifically with the targeted biomolecule of interest, mostly through the cavity approach, and transduced via the TFET platform as a change in the electrical signals [21].

The remaining part of the paper is organised as follows. Section 2 explains the architecture of the device and simulation setup. Section 3 describes the results and discussion. Sections 4, finally summarises the Letter with the conclusion.

2. Device structure and simulation setup: Fig. 1 shows the cross-sectional view of (Fig. 1a) conventional dual-gate dielectric-modulated (DG DM)-TFET as a biosensor and (Fig. 1b) dual-gate source electrode dielectric-modulated (DG SE DM)-TFET as a biosensor. For both the devices, the design parameters considered are shown in Table 1. Simulation has been performed using Silvaco Atlas simulator, for this non-local BTBT model and bandgap narrowing (BGN) model is considered for the calculation of the tunnelling rate of charge carriers [19, 24, 25] in the simulation. Shockley–Read–Hall recombination and Auger recombination is activated by SRH and AUGER parameter, respectively [25, 26]. Trap-assisted tunnelling (TAT) model [26, 27] is incorporated to calculate the effect of the high electric field on drain current. As the device size scale down to the sub 10 nm regime it is mandatory to consider the quantum effect for this, quantum confinement model (Hansch's model) [25, 27] is considered. Along with this, the Wentzel–Kramer–Brillouin approximation and the self-consistent coupled Schrodinger–Poisson model [26, 27] considered to calculate tunnelling probability.

3. Results and discussion: This section of Letter shows the comparative picture of performance and sensitivity analysis of DG DM-TFET and DG SE DM-TFET biosensor. For performance analysis of devices, various characteristics such as energy band diagram, surface potential, e-tunnelling rate and current voltage characteristics are investigated.

3.1. Performance analysis of device with dielectric variation in cavity region: Figs. 2a and b show the surface potential of the device along the device length for different dielectric constant. In ON state of the device, as the biomolecules enter into the

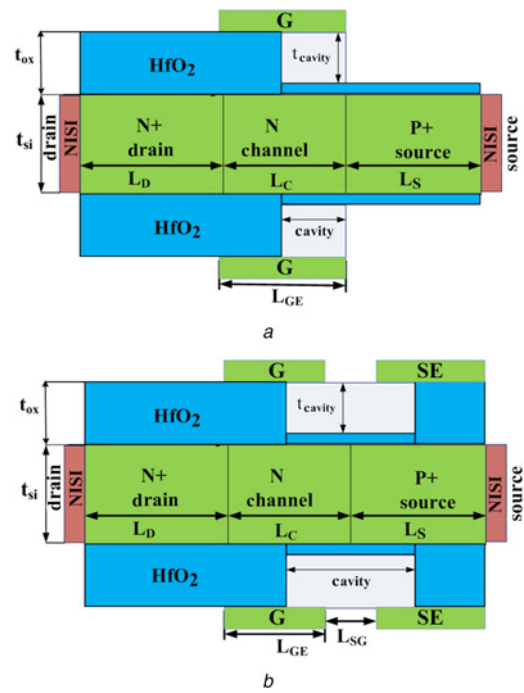


Fig. 1 Device architecture for
a Conventional DG DM-TFET biosensor and
b Proposed DG SE DM-TFET biosensor

Table 1 Parameter used for simulation

Parameters	Symbols	Conventional	Proposed
drain doping, cm ⁻³	N_A	1×10^{20}	1×10^{20}
source doping, cm ⁻³	N_D	1×10^{20}	1×10^{20}
channel doping, cm ⁻³	N_A	1×10^{17}	1×10^{17}
drain length, nm	L_D	100	100
source length, nm	L_S	100	100
channel length, nm	L_C	50	50
silicon thickness, nm	t_{si}	10	10
oxide thickness, nm	t_{ox}	6	6
gate-to-source electrode space, nm	L_{SG}	—	8
gate electrode work function, eV	ϕ_G	4.5	4.5
source electrode work function, eV	ϕ_{SE}	—	4.5
voltage at source electrode, V	V_{SE}	—	-1.2
length of cavity, nm	L_{Cavity}	15	30
height of cavity, nm	t_{Cavity}	5.5	5.5

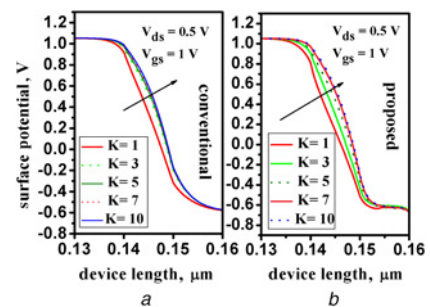


Fig. 2 Effect of dielectric variation on the surface potential of
a Conventional device and
b Proposed device

cavity, it increases the dielectric constant and increases coupling between the gate electrode and channel regions. Therefore, the increment is observed in the surface potential of both devices but DG SE DM-TFET shows a large increment in comparison to conventional device because in DG SE DM-TFET biomolecules enter into the source cavity region and increases the concentration of holes. Higher hole concentration creates an abrupt junction profile and increases the surface potential at source–channel junction more in comparison to DG DM-TFET device. As the surface potential increases with an increase in dielectric constant and pushes the energy bands of channel region more and more as shown in Figs. 3a and b. From Figs. 3a and b, it can be seen that DG SE DM-TFET showing more band bending variation due to variation in dielectric constant in comparison to the conventional device.

Further, Fig. 4 shows the electron tunnelling rate with the variation of the dielectric constant in the cavity region. As the value of K increases, the band bending increases and reduces the barrier width at the source–channel junction. So the tunnelling rate of electron increases for both the devices, but the more increment is observed in DG SE DM-TFET, which shows better sensitivity due to the presence of biomolecules of different properties. Furthermore, Figs. 5a and b show the electron current density, which is also showing higher sensitivity in DG SE DM-TFET against the variation in dielectric constant due to higher tunnelling rate. Consequently, the same variation is observed in the I_{ds} – V_{gs} characteristics as shown in Figs. 6a and b. It is essential to describe the sensitivity of the device to show the usefulness of the device. The sensitivity of the devices is calculated as

$$S_{I_{ds}} = \left(\frac{I_{D,bio} - I_{D,air}}{I_{D,air}} \right) \quad (1)$$

The sensitivity of the devices to drain current, against the variation of the dielectric constant in the cavity region, is shown in

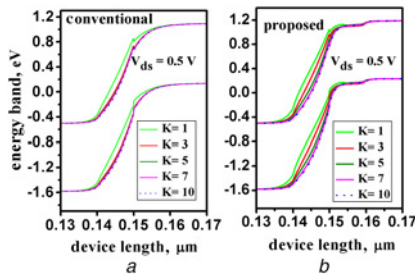


Fig. 3 Effect of dielectric variation on energy band diagram of
a Conventional device and
b Proposed device

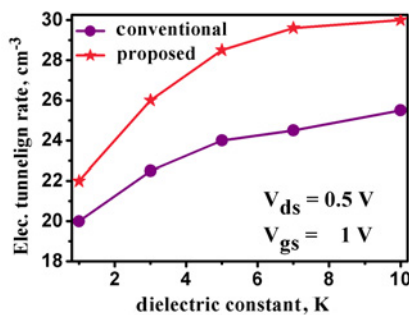


Fig. 4 Effect of dielectric variation on electron tunnelling rate for both devices

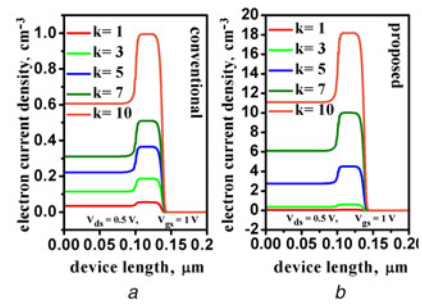


Fig. 5 Effect of dielectric variation on electron current density of
a Conventional and
b Proposed

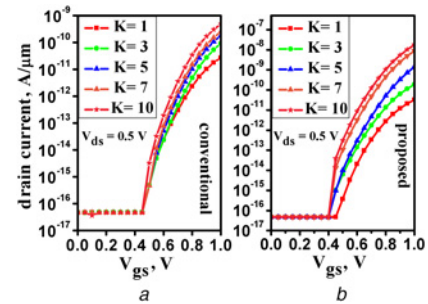


Fig. 6 Effect of dielectric variation on I_{ds} – V_{gs} characteristics of
a Conventional and
b Proposed

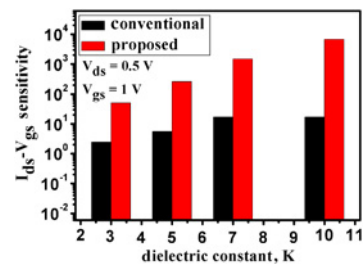


Fig. 7 Sensitivity of the devices in terms of I_{ds} – V_{gs} characteristics for the different dielectric constant of both devices

Fig. 7, where higher sensitivity is observed for DG SE DM-TFET, because the drain current in DG SE DM-TFET is depended upon the dielectric constant under the gate electrode region and dielectric under the source electrode region. Therefore, the nanogap cavity for the proposed device is created from a gate oxide region to source oxide region. Thus, the variation in drain current of DG SE DM-TFET is more in comparison to the conventional device, which shows better sensitivity for sensing biomolecules by DG SE DM-TFET than DG DM-TFET as shown in Fig. 7. The speed of the sensor to sense the presence of the biomolecule is also matters and it depends upon the SS of the device. From Fig. 8a, it can be observed that the SS of DG SE DM-TFET is lower in comparison to a conventional device for all value of K , therefore, it has the higher speed for sensing the biomolecule in cavity region. The variation in SS of DG SE DM-TFET is more due to increase in abruptness at source/channel junction, because as value of K increases it increases accumulation of holes under the source electrode in the source region, which causes an increment in abruptness at source/channel junction, hence the higher sensitivity is observed in Fig. 8b.

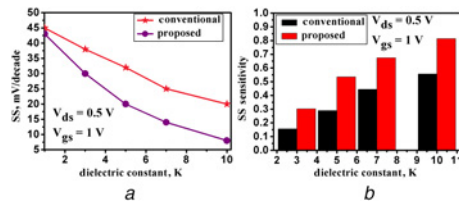


Fig. 8 Impact of dielectric variation on
a SS for both devices
b SS sensitivity for both devices

Furthermore, comparative performance of both devices in terms of output characteristics of the devices are carried out for different dielectric constant as shown in Figs. 9a and b. The output characteristics are plotted on the log scale and showing large variation in drain current with the variation in dielectric constant. Fig. 10a shows the sensitivity of the device for output current and it can be perceived that DG SE DM-TFET has higher sensitivity in comparison to DG DM-TFET for dielectric variation. Further, it can be observed that the ratio of ON and OFF current ratio is higher in the proposed device it can easily sense and recognise, which is also shown higher sensitivity as shown in Fig. 10b.

The transit time is the most important property of the biosensor, which decides the sensing speed of the biosensor, where it is defined as Transit Time(τ) = $1/2\pi f_T$. In other words, it can also be defined as the time required by the carriers to reach from the source region to the drain regions. In the DG SE DM-TFET, the cavity is extended into the source oxide region, therefore, as the dielectric constant increases, it increases the hole concentration. Increases in hole concentration create abrupt junction which is helpful for enhancing the transconductance of the device because the transconductance improves the cut of the frequency of the device and reduces the transit time of the device. Figs. 11a and b show the transit time of both the devices and it shows that DG

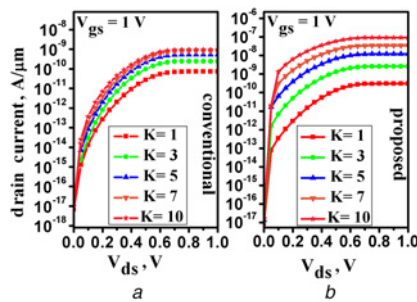


Fig. 9 Effect of dielectric variation on I_{ds} - V_{ds} characteristics of
a Conventional and
b Proposed

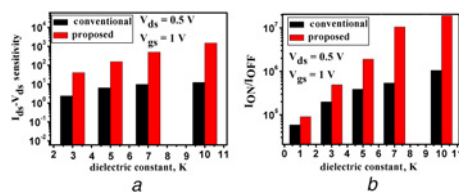


Fig. 10 Impact of dielectric variation on
a Sensitivity of the devices in terms of I_{ds} - V_{ds}
b I_{ON}/I_{OFF} ratio for different dielectric constant

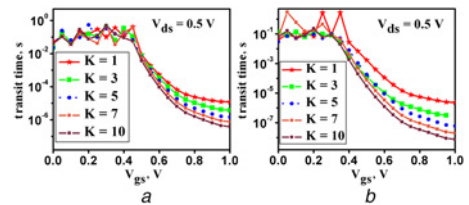


Fig. 11 Effect of dielectric variation on transit time for
a Conventional and
b Proposed

SE DM-TFET required less time to sense the biomolecule in the cavity region as compared to DG DM-TFET.

3.2. Performance analysis of device with charge density variation in cavity region: The detection of the charged molecule is another advantage of TFET-based biosensor over FET biosensor. Therefore, the performance is analysed for different density of charged molecule in the cavity region. For this, the surface potential in Figs. 12a and b and energy band diagram in Figs. 13a and b is shown, which shows large variation due to changes in charge density present in the cavity region. Due to higher surface potential variation and band bending in the channel region, large variation is observed in the electron current density of DG SE DM-TFET which can easily be recognised as shown in Figs. 14a and b. For showing the effect of a charged molecule inside the cavity electron tunnelling rate is demonstrated in Fig. 15, where it is observed that the electron tunnelling rate is higher for the DG SE DM-TFET as well as a percentage variation in the tunnelling rate, is more in DG SE DM-TFET in comparison to DG DM-TFET. Further, I_{ds} - V_{gs} characteristics for different charge molecules are shown in

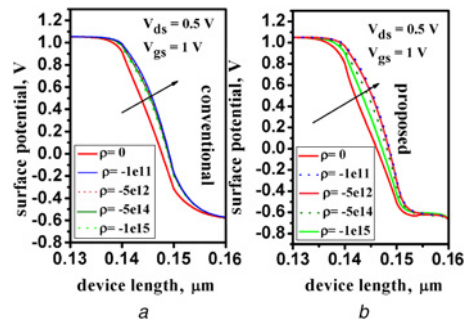


Fig. 12 Impact of charge of biomolecules on the surface potential of
a Conventional and
b Proposed

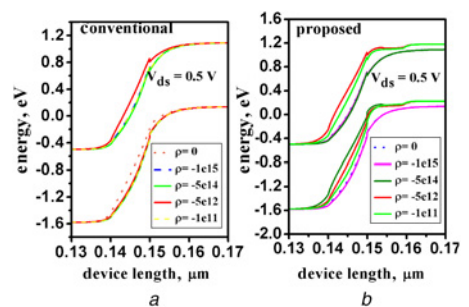


Fig. 13 Impact of charge of biomolecules on energy band diagram of
a Conventional and
b Proposed

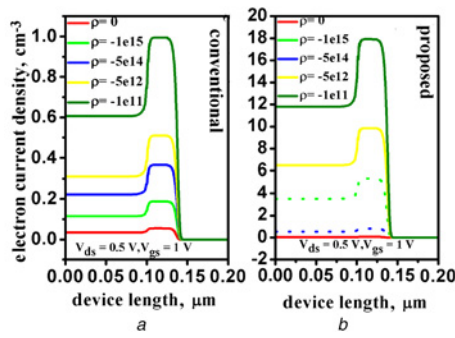


Fig. 14 Impact of charge of biomolecules on electron current density of
a Conventional and
b Proposed

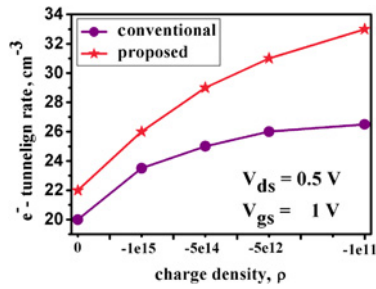


Fig. 15 Impact of charge of biomolecules on electron tunnelling rate of both devices

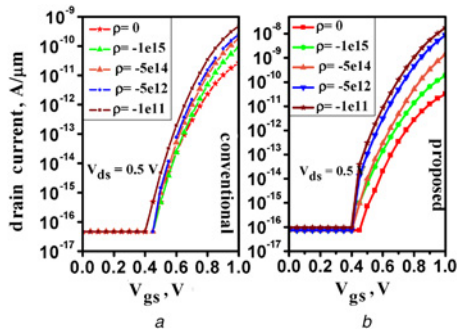


Fig. 16 Impact of charge of biomolecules on I_{ds} - V_{gs} characteristics of
a Conventional and
b Proposed

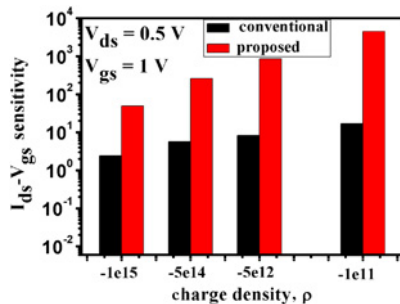


Fig. 17 Sensitivity of the devices in terms of I_{ds} - V_{gs} characteristics for different density of charge biomolecules for both devices

Figs. 16a and b, it can be seen in the figure that DG SE DM-TFET showing drain current variation of three decades in comparison to DG DM-TFET of one decade variation when the

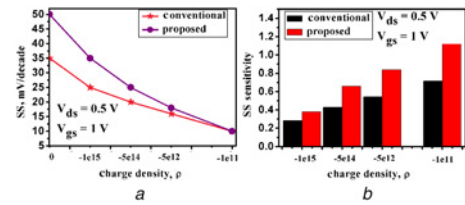


Fig. 18 Impact of charge of biomolecules on
a SS for both devices
b SS sensitivity for both devices

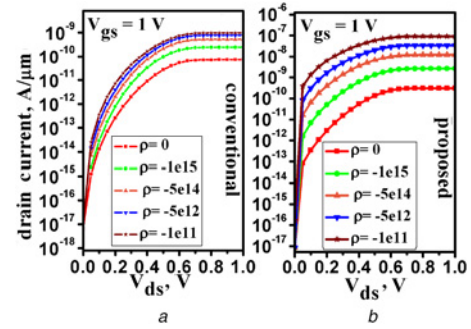


Fig. 19 Effect of charge of biomolecules on I_{ds} - V_{ds} characteristics of
a Conventional and
b Proposed

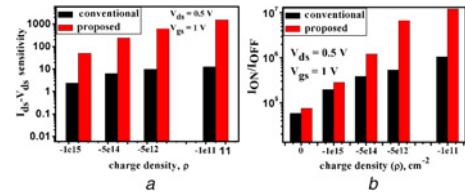


Fig. 20 Impact of charge of biomolecules on
a Sensitivity of the devices in terms of I_{ds} - V_{ds} characteristics
b I_{ON} - I_{OFF} ratio for different dielectric constant

charge of biomolecule changes from $\rho = 0$ to $\rho = -1e^{11}$. Therefore, to show the effectiveness of the newly designed cavity in DG SE DM-TFET Fig. 17 shows the sensitivity of both devices in terms of I_{ds} - V_{gs} variation for different charge molecules in the cavity region, which is higher for DG SE DM-TFET.

Furthermore, to check the sensitivity of devices, SS is calculated and presented in Fig. 18a and sensitivity due to the different charged molecule is shown in Fig. 18b, variation in SS is large for DG SE DM-TFET than DG DM-TFET, therefore, proposed device has a higher detection speed of charge biomolecule than the conventional device. The output characteristics of the devices for the different charge density of biomolecule are presented in Figs. 19a and b, here 2.5 decades of drain current variation are observed in DG SE DM-TFET in comparison to DG DM-TFET variation of 1 decade, therefore, it can be stated that the sensing capability of DG SE DM-TFET is much better in comparison to DG DM-TFET as shown in Fig. 20a. The impact of charged biomolecules in the cavity region is also demonstrated by calculated the ON-OFF current ratio (I_{ON} - I_{OFF}) as shown in Fig. 20b, it shows that the proposed device is having more variation in I_{ON} - I_{OFF} ratio in comparison to the conventional device. A comparative picture of sensitivity and sensing speed is shown in Tables 2 and 3, respectively.

Table 2 Comparison picture of sensitivity in V-DMTFET [18] and proposed device

Devices	I_d - V_g sensitivity for dielectric		I_d - V_g sensitivity for charge density		SS sensitivity for dielectric	
	K	Sensitivity	Charge density	Sensitivity	K	Sensitivity
V-DMTFET	2	10	$-1e^{11}$	5	2	0.2
	4	100	$-5e^{12}$	2	4	0.3
proposed	2	50	$-1e^{11}$	250	2	0.35
	4	150	$-5e^{12}$	200	4	0.55

Table 3 Comparison of sensing speed in the conventional and proposed device

Dielectric constant, K	Transient delay (conventional), s	Transient delay (proposed), s
1	1×10^{-5}	5×10^{-6}
3	5×10^{-6}	5×10^{-7}
5	1×10^{-6}	8×10^{-8}
7	5×10^{-7}	4×10^{-8}
9	9×10^{-7}	9×10^{-9}

4. Conclusion: In this Letter, we have proposed a new concept of cavity design of the conventional TFET device for the detection of the neutral/charged biomolecule. The device electrostatics and electrical parameters present that additional electrode with negative voltage over the source region overcomes the solubility limit of the silicon. Further, the extended cavity in the source region improved the sensitivity and sensing the speed of the TFET biosensor, drain current, the I_{on}/I_{off} ratio transient time, electron tunnelling rate and so on are carried out to show the impact of variation of a biomolecule in the cavity. Thus, the proposed device shows higher sensitivity and sensing speed in comparison to conventional TFET biosensor.

5 References

- Barbaro M., Bonfiglio A., Raffo L.: 'A charge-modulated FET for detection of biomolecular processes: conception, modeling, and simulation', *IEEE Trans. Electron Devices*, 2006, **53**, (1), pp. 158–166
- Kim C.-H., Jung C., Park H.G., *ET AL.*: 'Novel dielectric modulated field-effect transistor for label-free DNA detection', *Biochip J.*, 2008, **2**, (2), pp. 127–134
- Kim J.Y., Ahn J.H., Choi S.J., *ET AL.*: 'An underlap channel-embedded field-effect transistor for biosensor application in watery and dry environment', *IEEE Trans. Nanotechnol.*, 2012, **11**, (2), pp. 390–394
- Gao X.P.A., Zheng G., Lieber C.M.: 'Subthreshold regime has the optimal sensitivity for nanowire FET biosensors', *Nano Lett.*, 2010, **10**, (2), pp. 547–552
- Kannan N., Kumar M.J.: 'Dielectric-modulated impact-ionization MOS transistor as a label-free biosensor', *IEEE Trans. Electron Devices*, 2013, **34**, (12), pp. 1575–1577
- Im H., Huang X.-J., Gu B., *ET AL.*: 'A dielectric-modulated field-effect transistor for biosensing', *Nature Nanotechnol.*, 2007, **2**, pp. 430–434
- Gautam R., Saxena M., Gupta R.S., *ET AL.*: 'Numerical model of gate-all-around MOSFET with vacuum gate dielectric for biomolecule detection', *IEEE Electron Device Lett.*, 2012, **33**, (12), pp. 1756–1758
- Narang R., Saxena M., Gupta M.: 'Comparative analysis of dielectric-modulated FET and TFET-based biosensor', *IEEE Trans. Electron Devices*, 2015, **14**, (3), pp. 427–435
- Kanungo S., Chattopadhyay S., Gupta P.S., *ET AL.*: 'Comparative performance analysis of the dielectrically modulated full-gate and short-gate tunnel FET-based biosensors', *IEEE Trans. Electron Devices*, 2015, **62**, (3), pp. 994–1001
- Narang R., Reddy K.V.S., Saxena M., *ET AL.*: 'A dielectric-modulated tunnel-FET-based biosensor for label-free detection: analytical modeling study and sensitivity analysis', *IEEE Trans. Electron Devices*, 2012, **59**, (10), pp. 2809–2817
- Boucart K., Ionescu A.M.: 'Double-gate tunnel FET with high-gate dielectric', *IEEE Trans. Electron Devices*, 2007, **54**, (7), pp. 1725–1733
- Narang R., Saxena M., Gupta R.S., *ET AL.*: 'Dielectric modulated tunnel field-effect transistor a biomolecule sensor', *IEEE Electron Device Lett.*, 2012, **33**, (2), pp. 266–268
- Kanungo S., Chattopadhyay S., Gupta P.S., *ET AL.*: 'Study and analysis of the effects of SiGe source and pocket-doped channel on sensing performance of dielectrically modulated tunnel FET-based biosensors', *IEEE Trans. Electron Devices*, 2016, **63**, (6), pp. 2589–2596
- Sarkar D., Banerjee K.: 'Proposal for tunnel-field-effect-transistor as ultra-sensitive and label-free biosensors', *Appl. Phys. Lett.*, 2012, **100**, pp. 143108-1–143108-4
- Lanuzza M., Strangio S., Crupi F., *ET AL.*: 'Mixed tunnel FET/MOSFET level shifters: a new proposal to extend the tunnel fet application domain', *IEEE Trans. Electron Devices*, 2015, **62**, (12), pp. 3973–3979
- Saurabh S., Kumar M.J.: 'Novel attributes of a dual material gate nanoscale tunnel field-effect transistor', *IEEE Trans. Electron Devices*, 2010, **58**, (2), pp. 404–410
- Parihar M.K., Kranti A.: 'Enhanced sensitivity of double gate junctionless transistor architecture for biosensing applications', *Nanotechnology*, 2015, **26**, (14), pp. 1–8
- Verma M., Tirkey S., Yadav S., *ET AL.*: 'Performance assessment of a novel vertical dielectrically modulated TFET-based biosensor', *IEEE Trans. Electron Devices*, 2017, **63**, (9), pp. 3841–3848
- Soni D., Sharma D., Yadav S., *ET AL.*: 'Performance improvement of doped TFET by using plasma formation concept', *Superlattices Microstruct.*, 2017, **113**, pp. 97–109
- Zhang S., Geryak R., Geldmeier J., *ET AL.*: 'Synthesis, assembly, and applications of hybrid nanostructures for biosensing', *Chem. Rev.*, 2017, **117**, pp. 12942–13038
- Wang B., Cancilla J.C., Torrecilla J.S., *ET AL.*: 'Artificial sensing intelligence with silicon nanowires for ultrasensitive detection in the gas phase', *Nano Lett.*, 2014, **14**, pp. 933–938
- Kalantar-Zadeh K., Berean K.J., Ha N., *ET AL.*: 'A human pilot trial of ingestible electronic capsules capable of sensing different gases in the gut', *Nature Electron.*, 2018, **1**, pp. 79–87
- Kalantar-Zadeh K., Yao C.K., Berean K.J., *ET AL.*: 'Intestinal gas capsules: a proof-of-concept demonstration', *Gastroenterology*, 2016, **150**, pp. 37–39
- Kanungo S., Chattopadhyay S., Gupta P.S., *ET AL.*: 'Comparative performance analysis of the dielectrically modulated full gate and short-gate tunnel FET-based biosensors', *IEEE Trans. Electron Devices*, 2015, **62**, (3), pp. 994–1001
- 'ATLAS device simulation soft' (Silvaco, Santa Clara, CA, USA, 2012)
- Padilla J.L., Gamiz F., Godoy A.: 'Impact of quantum confinement on gate threshold tage and subthreshold swings in double-gate tunnel FETs', *IEEE Trans. Electron Devices*, 2012, **59**, (12), pp. 3205–3211
- Hansch W., Vogelsang T., Kircher R., *ET AL.*: 'Carrier transport near the Si/SiO₂ interface of a MOSFET', *Solid State Electron.*, 1989, **32**, (10), pp. 839–849